Available online at www.sciencedirect.com
SCIENCE DIRECT®
ELSEVIER
Progress in Materials Science 49 (2004) 389–410
Progress in Materials Science
www.elsevier.com/locate/pmatsci

Phase relations and precipitation in Al–Mg–Si alloys with Cu additions☆

D.J. Chakrabarti[a], David E. Laughlin[b,*]

[a]*Alcoa Technical Center, Alcoa Center, PA 15069, USA*
[b]*Department of Materials, Carnegie Mellon University, Pittsburgh, PA 15213, USA*

Abstract

Application prospects in automotive industry have led to extensive studies on 6xxx alloys in recent years. These alloys often contain Cu in varying amounts. This leads to the formation of the quaternary Al–Mg–Si–Cu family of alloys that may exist either as a 6xxx or a 2xxx alloy. These alloys have distinctive properties in part due to the occurrence of a phase, designated as Q, which is stable only as a quaternary compound with variously reported stoichiometry. In this paper we first review the equilibrium phase field of various Al–Mg–Si–Cu alloys, noting the many important commercial alloys that contain the Q phase as an equilibrium one. We review the metallographic and crystallographic aspects of the Q phase. One of the important precursors of the Q phase is the Q′ phase, and its crystallography and microstructural features are presented and discussed. Various other competing metastable phases in both ternary and quaternary systems are presented and an attempt is made to systematize their occurrence with respect to overall alloy composition. The metastable precursor phase Q′ has the same crystal system and similar composition as Q. Recent literature indicates that a phase with the same crystal system, orientation relations and lath morphology as Q′ is also found in ternary Al–Mg–Si alloys with Si contents in excess of the balanced composition. This phase is metastable and is replaced by the equilibrium β phase. Finally, all of these alloys have been reported to be strengthened primarily by β″ phase during artificial aging such as during paint bake (~180 °C). The source of such strengthening in quaternary alloys is critically analyzed in light of conflicting reports on the ubiquity of β″ phase and studies on the role of the Q′ and other likely metastable phases.

☆ This paper in honor of Professor T.B. Massalski is based partly on two earlier presentations on the topic by the authors published in: (1) "Automotive Alloys II", 1998, TMS, USA, pp. 27–44, and (2) International Conference in Aluminum Alloys 8, University of Cambridge, UK, July, 2002.

* Corresponding author. Tel.: +1-412-268-2706; fax: +1-412-2687169.
E-mail address: dl0p@andrew.cmu.edu (D.E. Laughlin).

0079-6425/03/$ - see front matter © 2003 Elsevier Ltd. All rights reserved.
doi:10.1016/S0079-6425(03)00031-8

Contents

1. Introduction

In this review we summarize some of our previous work on the phase equilibria, metastable phases, their sequence of precipitation and strengthening in Al–Mg–Si and Al–Mg–Si–Cu alloys [1–6]. The properties of 6xxx Al-Mg-Si alloys have been known to be influenced by the precursor phases to the equilibrium Mg_2Si (β). In many commercial 6xxx alloys, which often contain Cu in varying amounts (e.g. 6061) several other equilibrium phases coexist with β. One of them is the quaternary intermediate phase which has been given different designations and reported with different stoichiometries. Herein, we call this the Q phase. The Q phase is present as an equilibrium phase in many alloys based on the Al–Mg–Si–Cu system. This paper will identify the different equilibrium phase fields present in the Al–Mg–Si–Cu systems for different compositions, and relate them to the various commercial families of alloys. The morphology and crystallography of Q phase will also be reviewed.

The aging response in Al–Mg–Si–Cu alloys often appears to be quite complex owing to the occurrence of many intermediate phases. Application prospects of these alloys in the automotive industry have sparked considerable activities leading to the report of many different alloy compositions of both ternary alloys and quaternary alloys at different Cu levels. The precipitation events in the ternary 6xxx alloys represented by the Al–Mg–Si system was earlier reported to be: solid solution $\rightarrow$ GP $\rightarrow$ β″ $\rightarrow$ β′ $\rightarrow$ β [7–9]. The picture has since grown considerably more complex. Several additional clustering phases [10] and, in the presence of Cu, metastable

versions under different designations of the quaternary Q phase have been reported [1,4,11–15]. Metastable versions of Q in ternary Al–Mg–Si alloys with excess-Si compositions (over the Mg_2Si stoichiometry) have been also reported [12,16–18]. In addition, high resolution electron microscopy has exposed a plethora of new metastable phases and their varied precipitation sequences. Confusion is arising from the use at times of different nomenclatures by different researchers for the same phases. A logical framework which encompasses the metastable phase precipitation details in the 6xxx alloys is needed and will be addressed.

The prevailing viewpoint [3,10] ascribes strengthening in all these families of alloys to the β″ phase which occurs at peak age. However, other phases have been reported present together with β″ at peak age, in particular in Cu-containing quaternary alloys, while the relative β″ population is reported to vary, depending on the alloy composition [12,13]. The sources of strengthening in these families of alloys are critically analyzed using our results [6] as well as those found in the literature.

2. Equilibrium phase fields of Al–Mg–Si–Cu alloys

The Al–Mg–Si–Cu family of alloys is formed when Cu is added to the 6xxx series Al–Mg–Si alloys, or conversely, Si is added to the 2xxx series Al–Cu–Mg alloys. Thus, these quaternary alloys straddle both the 2xxx and 6xxx alloy compositions and do not have a separate designation in the Aluminum Association's scheme [19]. One important underlying common feature in all these alloys is the occurrence of a quaternary phase first experimentally observed in the Alcoa Laboratories by Dix et al., who designated it as the Al–Cu–Mg–Si phase [20]. The phase has since then been variously designated as either Q [21–24], h-AlCuMgSi [11] W [25], or λ [26].

Many commercial ternary Al–Mg–Si alloys have their compositions in a three-phase field (at normal aging temperatures) consisting of the equilibrium phases: primary aluminum, (Al), β and primary Si, (Si). On addition of Cu, the coexisting equilibrium three-phase fields expand into three tetrahedron composition spaces. A four-phase equilibrium is present inside each of these spaces consisting of the two common phases, namely (Al), and the quaternary intermediate phase Q, and two of the other three phases, namely θ ($CuAl_2$), β and (Si). This is schematically shown in the skeletal phase diagram representation in Fig. 1, modified from an earlier diagram by Collins (23). Three-phase fields in this diagram are schematically shown contained within the triangular faces, two-phase fields by compositions bound by the parallel lines and single phase fields as point compositions by the circles. Filled circles represent corners of the three four-phase tetrahedrons discussed above.

Fig. 1 shows that when Si is added to the Al–Cu–Mg alloys, the three-phase field consisting of (Al), θ and S expands into the tetrahedron consisting of (Al), θ, S and β phases at low Si. At higher Si, a cross over occurs to the tetrahedron in which Q replaces S, and the tetrahedron consists of the phases (Al), θ, β and Q, similar to those present when Cu is added to 6xxx alloys. We believe that this cross over from the tetrahedron phase field containing S to the tetrahedron phase field containing Q is reflected in the observed shift of the highest temperature endothermic peak from

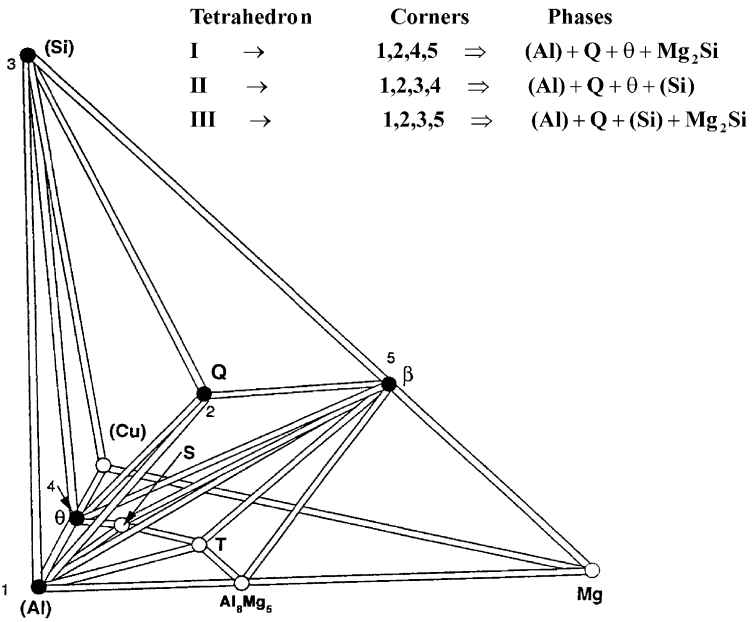

Fig. 1. Line diagram of stable equilibrium phase fields in Al–Mg–Si–Cu system at room temperature.

about 290 to 340 °C, when the Si addition to the Al–2Cu–0.9Mg alloy was increased from 0.25 to 0.5%, see Fig. 2 of Suzuki et al. [27]. In this paper only the cases of Cu additions to Al–Mg–Si will be discussed, although equivalent phase relations and property results would also be present in Al–Cu–Mg alloys with Si additions.

In the quaternary Al–Mg–Si–Cu system when the Mg/Si ratio[1] is greater than about 1, the compositions at artificial aging temperatures have been calculated [28] to lie in Tetrahedron I (Fig. 1), which has the coexisting phases, (Al), Q, θ and β. When Mg/Si <1, the compositions occupy Tetrahedron II, having the coexisting phases, (Al), Q, θ and (Si). The Tetrahedron III composition field is occupied when the Cu level is low, the value of which varies with the Mg and Si, but is generally less than 0.2–0.5%. A clearer view of the tetrahedral phase fields is shown in a simplified schematic projection (not to scale) of the (Al) corner of the tetrahedron onto the Q corner of the tetrahedron whereby the tetrahedrons are projected in two dimensions as triangular fields, as shown in Fig. 2.

An interesting aspect of the composition-phase field relationship is immediately apparent. In the Al–Mg–Si alloys, a Mg/Si ratio of 1.73:1 (corresponding to the 2:1 stoichiometry for Mg_2Si) is assumed for the formation of β. If the ratio is less than 1.73:1 the alloy is designated as an "excess Si" one. Studies by Edwards et al. [29], however, showed that for the metastable precursor phases, the appropriate composition ratio should be more like 1:1. In the Al–Mg–Si–Cu system, the Mg/Si ratio defining the phase boundary between tetrahedrons I and II appears to be also close

[1] All compositions in this paper are expressed in weight percentage.

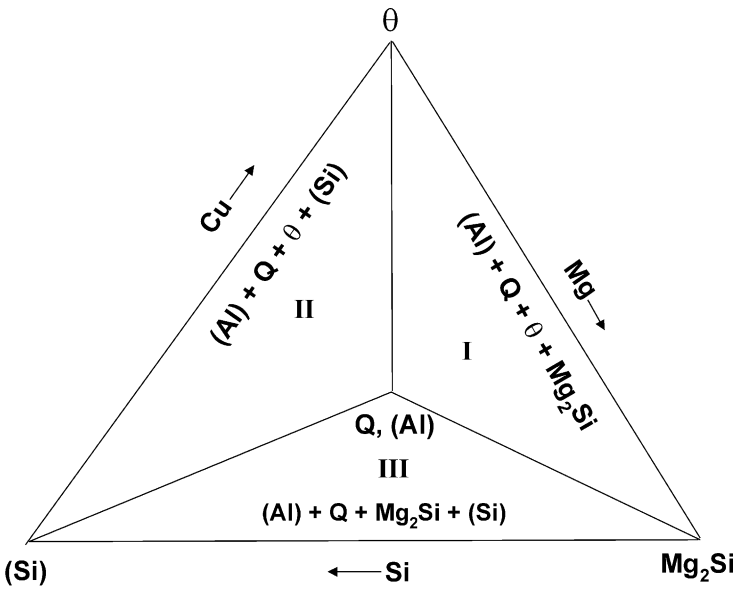

Fig. 2. Al–Mg–Si–Cu alloys grouped by phase field occupancy on a pseudo-projection of the four-phase-field tetrahedrons. The vertical line represents alloys with Mg/Si = 1.

to 1:1 [28]. Thus of all the "excess Si" compositions of auto-body sheet (ABS) alloys, only those having Mg/Si < 1 belong to the Tetrahedron II phase field. Put another way, the stabilization of (Si) (tetrahedron II) in preference to Mg_2Si (tetrahedron I) requires higher Si in the quaternary alloy than assumed in the ternary alloy.

In regard to the composition effect on the relative phase stability, our equilibrium diagram calculations and experiments [28,30] indicate certain definite trends. In both Tetrahedron I and II, Cu has the strongest stabilizing effect on the amount of θ and much less on the other coexisting phases. Increasing Si strongly increases the amount of Q in Tetrahedron I, and the amount of (Si) in Tetrahedron II. Increasing Mg increases Mg_2Si in Tetrahedron I and Q in Tetrahedron II. It is important to note that although the addition of Cu to Al–Mg–Si alloys introduces the Q phase, it also introduces θ and modifies the relative amounts of (Si) and Mg_2Si due to a change in the coexisting equilibrium phase fields. However, the impact of Cu addition on the relative volume fractions is much stronger on θ than on Q.

3. The ubiquity of Q and the coexisting equilibrium phases

The quaternary Q phase is present as an equilibrium phase at most of the compositions in the Al–Mg–Si–Cu system. For example, Q is present in all three tetrahedrons phase fields which, as shown in Fig. 1, occupy the bulk of the composition fields at normal aging temperatures. It is also obvious from Fig. 1 that the Q phase

cannot coexist in equilibrium with the S or T phases commonly observed in the Al–Cu–Mg system, or with the Al_8Mg_5 phase in the Al–Mg system.

Each tetrahedron being identified with specific phase combinations, therefore, shares the particular engineering properties associated with the alloys in its composition field. The distribution of some of the common commercial alloys in the three tetrahedron phase fields is listed in Table 1.

Fig. 3 shows how specific changes in composition (often in terms of Mg/Si ratio), can change the alloy types. The composition alterations change the alloy type by shifting from one tetrahedron four-phase field to another four-phase field in a quaternary alloy. It is also possible for a quaternary alloy existing in a four-phase field to become a ternary alloy in a three-phase field by the elimination of one of its components (e.g., 2017 becomes 2024 with the elimination of Si). It may be noted that the switch from tetrahedron I to II occurs with a decrease of Mg or an increase of Si or their combinations. The reverse composition relations hold for a switch from tetrahedron II to I. Also, chronological ordering of the alloys under each column shows that the Si content in the ABS alloys (under tetrahedron II) has progressively increased.

4. Crystal structure and microstructure of the Q phase

The structure and composition of the Q phase have been variously reported [11,21–26]. Phragmen determined the phase to be hexagonal [11]. The most detailed descriptions of the structure are given by [31] and [32]. Arnberg et al. [31] describes the Q phase as based on Th_7S_{12} structure in which Si atoms take the place of the Th atoms and Al and Mg atoms are randomly placed on the sites occupied by S in the

Table 1
Examples of common Al–Mg–Si–Cu alloys and associated four-phase equilibrium fields at normal aging temperatures[a]

Tetrahedron			Composition (wt.%)			Application
I	II	III	Mg	Si	Cu	
2017			0.40–0.8	0.2–0.8	3.50–4.5	(a)
2036			0.30–0.6	0.5[c]	2.20–3.0	(c1)
6061		6061[b]	0.80–1.2	0.4–0.8	0.15–0.4	(a,c3)
6013			0.80–1.2	0.6–1.0	0.60–1.1	(a, b)
	2014		0.20–0.8	0.5–1.2	3.90–5.0	(a, b)
	2008		0.25–0.5	0.5–0.8	0.70–1.1	(c1)
	6009	6009[b]	0.40–0.8	0.6–1.0	0.15–0.6	(c1, c2)
	6111		0.50–1.0	0.7–1.1	0.50–0.9	(c1)
		6016	0.25–0.6	0.9–1.3	0.20[c]	(c1, c2)
		6022	0.45–0.7	0.8–1.5	0.01–0.11	(c1)

[a] Stable phases: **I**: (Al) + Q + Mg2Si + θ; **II**: (Al) + Q + (Si) + θ; **III**: (Al) + Q + Mg2Si + (Si) (a): general; (b): aerospace; (c1): auto exterior, (c2): auto inner, (c3): auto extrusion.

[b] Indicates tetrahedron occupancy at low Cu end of the composition range.

[c] Indicates maximum; no lower limits.

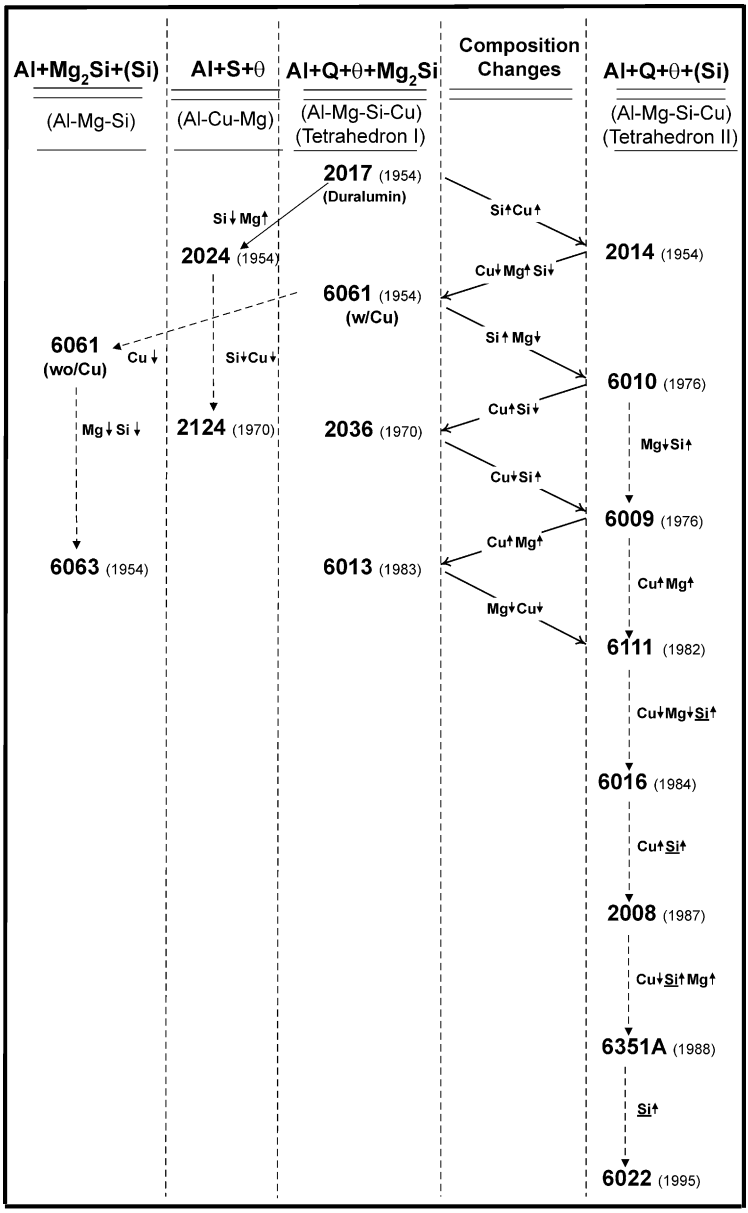

Fig. 3. Commercial Al–Mg–Si–Cu alloys grouped in different phase fields. The shift from one phase field to another with composition changes is shown by the slanting arrows. The elements which change going from one alloy to another are indicated between the alloy numbers. The alloys are arranged in each column in the chronological order of their development. Registration dates for the alloys with The Aluminum Association are shown within parentheses.

prototype structure. In addition, Cu atoms were thought to be placed at other sites that are not occupied in the Th_7S_{12} structure. This structure belongs to the hexagonal system [11] and has the space group $P\bar{6}$. The Q phase has lattice parameters $c = 0.405$ nm and $a = 1.04$ nm, has 21 atoms in a unit cell and its Pearson symbol is hP21 [33], if we use the structure proposed by Arnberg et al. [31]. The exact composition of the phase is unknown but has been stated as $Al_5Cu_2Mg_8Si_6$ [11], $Al_4CuMg_5Si_4$ [34], $Al_4Cu_2Mg_8Si_7$ [31] and $Al_3Cu_2Mg_9Si_7$ [32].

Q formed during solidification from the liquid has a complex honeycomb type morphology as shown in the secondary electron SEM image for a 2014 sample in Fig. 4. The optical microstructure of Q appeared as a very fine eutectic structure, see Fig. 5. The as-cast Q phase morphology changes with long thermal exposure during homogenization, and the Q phase may also precipitate in the solid state during high temperature anneals. In these cases Q often forms as round or oval particles at the grain boundaries [35].

5. Metastable phases and the Q′ precursor phase

The tetrahedron phase fields discussed above refer to the equilibrium phases. They do not predict the metastable phases that may occur during artificial aging. However, the equilibrium phase field information is still very useful, as it may be used to predict the precipitation of those metastable phases that are the natural precursors to the equilibrium phases.

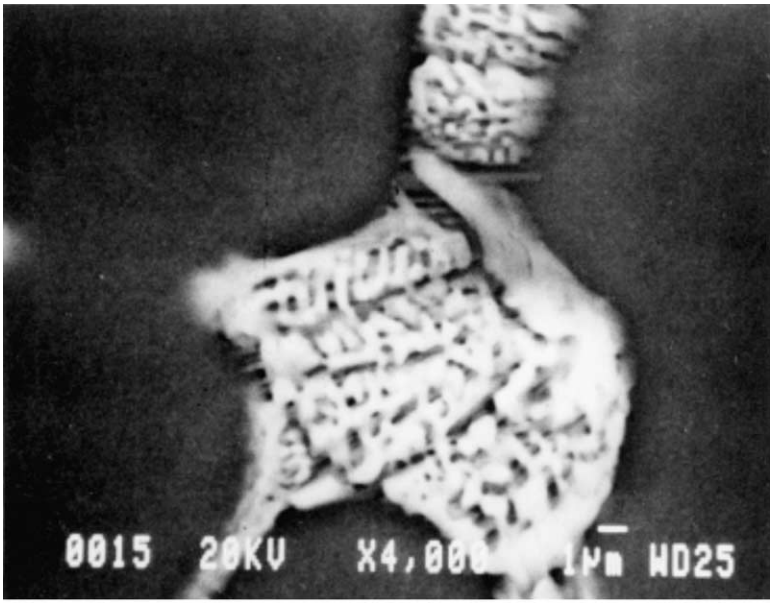

Fig. 4. SEM back-scattered electron image of 2014 ingot sample showing the honeycomb type structure of the Q phase.

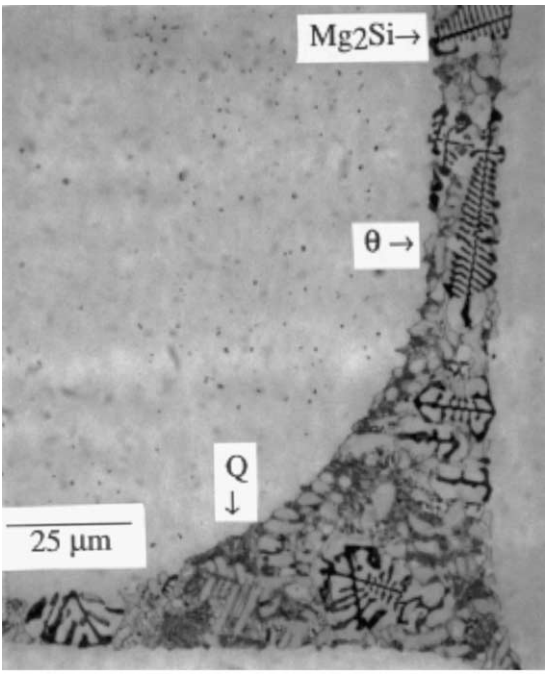

Fig. 5. Optical micrograph of an ingot sample with Mg/Si >1 (Mg: 1.15, Si: 0.92, Cu: 1.99) showing the Q phase with an intertwined structure.

Additional metastable phases may also form but certain generalizations may apply. For example, a metastable phase that has a crystal structure different from its equilibrium counterpart (e.g., θ′ or β′ in Table 2) could also form even when the equilibrium phase is absent. For a metastable phase that has the same crystal structure (i.e., same Bravais lattice *and* basis) and similar lattice parameters as its equilibrium counterparts (e.g., S′ and S in Table 2), if the metastable phase exists so should its equilibrium counterpart and vice versa. However, if only the crystal system is the same but not the crystal structure (due to a different basis) the equilibrium phase need not be present when its corresponding metastable phase is present. This helps us to understand how a ternary Q′-like phase (same Bravais lattice and lattice parameters) can exist in excess-Si ternary alloys in which the Q phase cannot exist (Q is a quaternary phase), see our discussion below the section on precipitation. The Q′-like ternary metastable phase has a different basis (no Cu) than the quaternary Q phase. The above arguments also would rule out the simultaneous occurrence in a quaternary system of the metastable S′ phase and the Q′ phase because S does not occur in any tetrahedron containing Q, (see Fig. 1).

In a previous paper [2] we questioned the absence of the Q′ phase and the presence of the S′ phase in the metastable phase diagram reported by Eskin [36]. However, recent studies have shown [3,10] that Q′ is not always present at peak aging in alloys which contain Q as an equilibrium phase. This explains why Q′ though expected was

Table 2
Crystallographic and morphological data of selected phases in aluminum alloys

Alloy system	Equilibrium phase (Bravais lattice)	Metastable phase		Metastable phase		
		Isostructural (with equilibrium phase)	Non-Isostructural	Bravais lattice (Shape)	Habit plane	Orientation relation
Al–Cu	θ (body centered tetragonal)	θ′		Body centered tetragonal (plate)	{100}	$[001]_{Al}//[001]\theta'$ $(100)_{Al}//(100)\theta'$
Al–Mg–Si	β (face centered cubic)	β′		Hexagonal (rod)	–	$[001]_{Al}//[0001]\beta'$ $(110)_{Al}//(10\bar{1}0)\beta'$
Al–Cu–Mg	S (side centered orthorhombic)	S′		Side centered orthorhombic (lath)	{210}	$[001]_{Al}//[001]_{S}'$ $(210)_{Al}//(010)_{S}'$
Al–Mg–Si–Cu	Q (hexagonal)	Q′		Hexagonal (lath)	{150}	$[001]_{Al}//[0001]_{Q}'$ $(020)_{Al}//(21\bar{3}0)_{Q}'$

not present in the high Si region of the diagram. We were incorrect to question the presence of S′ in the low Si quaternary alloys.

The metastable β″ has been observed to be the dominant intermediate phase present in the Al–Mg–Si and in some Al–Mg–Si–Cu alloys at early stages of aging. The β″ phase is needle shaped with the long axis along $<100>$ of the matrix Aluminum and its crystal structure is based on the monoclinic system [29]. After peak aging some of the needle shaped β″ precipitates are replaced by rod shaped phase β′. In the Al–Mg–Si–Cu alloys lath shaped precipitates appear at peak age and/or during overaging. A lath shaped phase was originally observed in 6061 alloy by Dumult et al. [1] who called it B′. This lath shaped precursor phase of the equilibrium Q phase has been designated as the Q′ phase [2] although other designations also exist. Its habit plane was determined to be {150} of the matrix, see Table 2.

Unlike the β′ to β transition which involves a change in crystal structure from hexagonal to the cubic CaF_2 structure, the Q′ phase maintains the same crystal structure and morphology as Q from peak age through the overaged conditions. Only its size increases [2]. Based on the above, this is one of those instances in which a precursor phase is crystallographically identical with the stable equilibrium phase.

In a later section we present a comprehensive summary of reported metastable phases and their sequence during the artificial aging process.

6. Crystallography of the Q′ phase

Dumult et al. [1] characterized a phase they called B′ as follows:

1. hexagonal with $c = 1.04$ nm and $a = 0.404$ nm
2. lath shaped with long directions parallel to the $<100>$Al
3. habit planes {150} of the Al matrix

This phase is really the coherent version of the equilibrium Q phase and is called Q′ in analogy with the well known designation of the coherent γ phase as γ′ in superalloys (or the S and S′ of Al–Cu–Mg alloys) when it forms with the above morphology and habit relations.

In Fig. 6 precipitates of the Q′ phase are shown in a bright field TEM micrograph of an overaged Al–Mg–Si–Cu alloy. The long dimensions of the precipitate phase lie along the $<100>$ matrix directions. The variants along the normal direction are rectangular in shape and have {150} habits with the Al matrix.

An indexed diffraction pattern for Q′ and Al is shown in Fig. 7. It can be seen that the $(21\bar{3}0)_{Q'}$ is parallel to the $(020)_{Al}$. The positions of the β′ spots are also included in Fig. 7. Their proximity to the Q′ spots could be a source of confusion in the identification of the Q′ phase.

The orientation relationship of $(21\bar{3}0)_{Q'}//(020)_{Al}$ is within 2° of that reported by [1]. Their relationship was derived from the habit planes of the precipitate assuming a good fit of lattice spacing. The perfect match in one direction (viz, the *c* axis of Q′ along the $<100>$ Al) is what gives rise to the long dimension of the lath parallel to one of the $<100>$ Al directions [37]. The repeat distance along the $<150>$ directions of the aluminum matrix is $0.404*\sqrt{26}/2 = 1.03$ nm. This is about the same as the lattice parameter of the Q′ phase. Hence during the solid state precipitation Q′ forms as a lath so as to minimize the misfit in its surface and hence its surface energy.

7. Precipitation of phases in Al–Mg–Si and Al–Mg–Si–Cu alloys

The phases and the sequence of their precipitation in the ternary Al–Mg–Si alloys have been extensively studied and reported in the literature. Information also exists

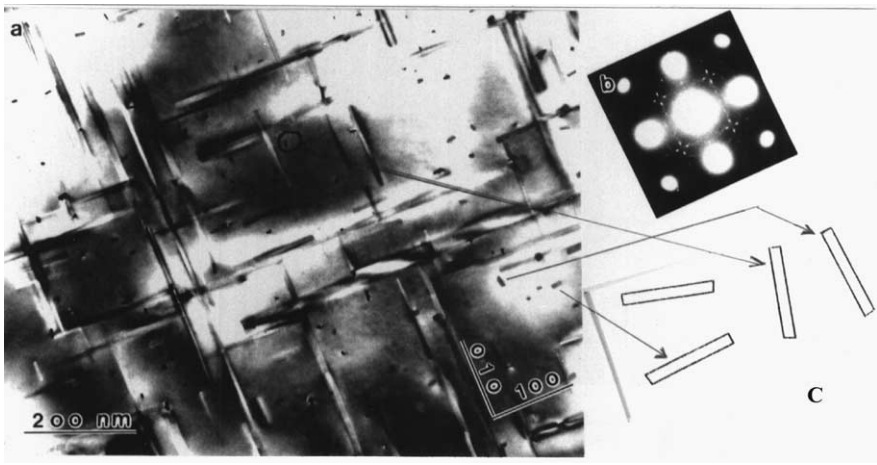

Fig. 6. TEM micrograph of an Al–Mg–Si–Cu sheet sample (overaged) at the [001] foil orientation: (a) BF (bright field), (b) SADP (selected area diffraction pattern), (c) schematic of the four end-on variants of the Q phase. Arrows indicate some of the variants in the BF image in (a) (from [2]).

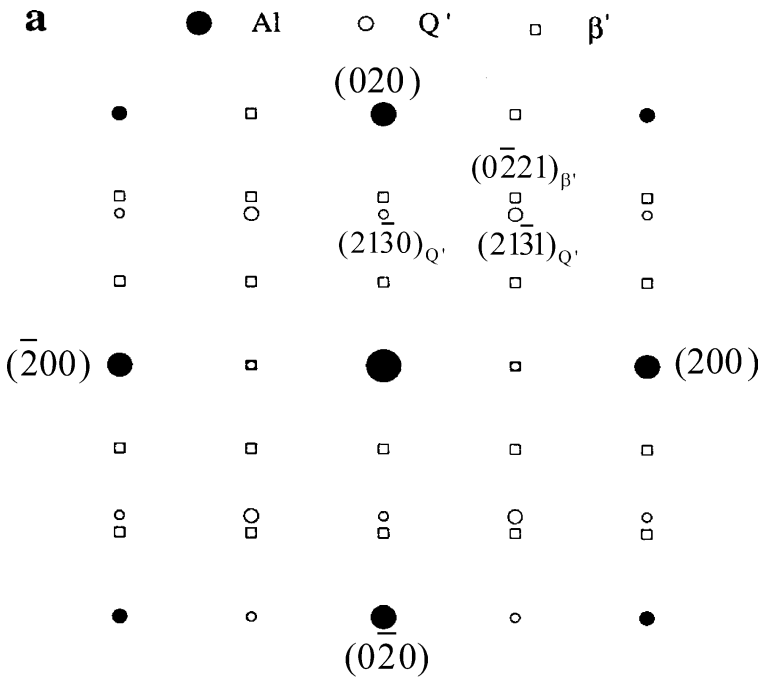

Fig. 7. A simulated diffraction pattern of β′ and Q′ in Al matrix with the orientation relationships of $[100]_{Al}//[0001]_{\beta'}$, $(020)_{Al}//(0\bar{2}20)_{\beta'}$ and $[100]_{Al}//[0001]_{Q'}$, $(020)_{Al}//(21\bar{3}0)_{Q'}$ (from [4]).

for the quaternary Al–Mg–Si–Cu alloys, though to a lesser extent. High resolution TEM studies in recent years have begun to introduce a plethora of metastable transition phases in both of the alloy systems. The sheer number of such new phases and the different designations used by the different investigators make the picture quite complex. We have systematized these results paying attention to those metastable phases that occur near the peak age and overage conditions, and the subsequent stable phases, see Table 3. The table lists in separate columns the precititating phases at peak age, and at three arbitrary, progressively overaged conditions (OA1, OA2, OA3), as well as the stable equilibrium phases. The systems under the "composition" are listed in terms of ternary versus quaternary, balanced (matching Mg_2Si stoichiometry) versus excess-Si (wt.% Mg <1.732*wt.% Si), high versus low excess-Si levels, and high versus low Cu levels in the quaternary composition. Each of the systems has noticeably different precipitation sequences. Also added in Table 3 are crystal system and lattice parameter information for the different phases according to the sequence in which they occur under the specific columns. Some of the phases shown within parentheses were added for completeness, but were not specifically mentioned in the referenced works.

The "Ternary Balanced" system is first discussed. Here the precipitates are the needle shaped β″ phase with a monoclinic structure at peak age, a mixture of β″ and hexagonal β′ progressively approaching β′ with overaging, and the equilibrium cubic

Table 3
Precipitation sequence and precipitate structure for different 6xxx alloy compositions

Composition	Peak age	OA 1	OA 2	OA 3	Equilibrium	Ref.
Ternary, excess-Si	β″ + β_d″			**M**	β	[12]
Ternary, excess-Si (low)	β″	β′ + **Type B**	**Type B + Type A**	**Type A + Type C**	β + (**Si**)	[16–18]
Ternary, excess-Si (high)	β″	β′ + **Type B**	**Type B + Type A**	**Type A + Type C**	**Si** + (β)	[16–18]
Ternary, balanced	β″	β′ + β″	β′	β′	β	[7–9]
Balanced + low Cu (1)	β″			**B**′ + β′	(β) + (**Q**) + (θ)	[1]
Balanced + low Cu (2)	β″ + **L**	**L** + β′ + β″	L + β′	β′ + **L**	β + λ **or Q** + (θ)	[12]
Balanced + high Cu	β″ + **L**	**L** + β″		**L**	λ **or Q** + β + (θ)	[12]
Excess-Si + low Cu	β″	β′ + Lath		β′ + **Q**′	β + **Si** + (**Q**)	[4]
Excess-Si + high Cu	β″	β″ + Lath	Lath	**Q**′	**Q** + **Si** + (θ)	[4]
Al–Mg–Si–Cu	β″ + **QP**	**QC** + **QP**		**Q**′	**Q** + (**Si** or β) + (θ)	[14,15]
	β″		β′		β	
	Monoclinic [12]		**Hexagonal** [12]		**Cubic** [12]	
	$a = 0.65$ nm, $b = 0.76$ nm		($a = 0.705$, $c = 0.405$) nm		$a = 0.642$ nm	
	$c = 0.405$ nm, $\gamma = 70^\circ$					
	L [12]			**Q**′	**Q**,γ	
	—			**Hexagonal** [2]	**Hexagonal** [2]	
	($a = 0.8$, $c = 0.7$) nm			($a = 1.03$, $c = 0.405$) nm	($a = 1.04$, $c = 0.405$) nm	
	β_d″			**M**		
	—			**Hexagonal** [38]		
				($a = 1.03$, $c = 0.405$) nm		
	QP	**QC**		**B**′		
	Hexagonal [14]	**Hexagonal** [14]		**Hexagonal** [1]		
	($a = 0.393$, $c = 0.405$) nm	($a = 0.67$, $c = 0.405$) nm		($a = 1.03$, $c = 0.405$) nm		
		Type B		**Type C**		
		Orthorhombic [16]		**Hexagonal** [16]		
		($a = 0.684$, $b = 0.793$, $c = 0.405$) nm		($a = 1.04$, $c = 0.401$) nm		
		Type A				
		Hexagonal [16]				
		($a = 0.405$, $c = 0.67$) nm				[reference]

β phase (Mg_2Si) [7–9], see Table 3. In the "Excess-Si + low Cu" case (1.28Si, 0.58Mg, 0.07Cu), β″ is observed at peak age, while on overaging a lath shaped phase coexists with the rod-like β′ phase (4). On longer overaging the lath phase displays the precipitate characteristics of the metastable Q′ phase. However, it is noteworthy that at equilibrium no Q is oberved and only β and Si phases are present. For "Excess-Si + high Cu" case (1.26Si, 0.55Mg, 0.91Cu), according to Miao et al. [4], β″ occurred at peak age while on overaging a lath like precipitate progressively dominated eventually leading at equilibrium to the Q phase together with the Si phase. Notably, the habit plane and orientation relations of the lath precipitates at the late stage of overaging resembled that of Q′, while they were different for the lath precipitates at the early stage, thus indicating that these were possible precursors to the Q′ phase.

As stated earlier, Dumolt et al. [1] reported for a "Balanced + low Cu(1)" alloy (0.6Si, 1Mg, 0.3Cu) the occurrence of β″ at peak age while on overaging a lath shaped phase designated by them as B′ appeared to coexist with the rod shaped β′ phase. The B′ phase for which they provided detailed information about the precipitate refers to the metastable precursor phase of Q, which is better termed Q′ [2]. For the "Balanced + low Cu (2)" system (0.65Si, 1Mg, 0.25Cu), a new lath-shaped phase L is cited by Segalowicz et al. [12] to occur at peak age along with β″, for which only the lattice parameter but no crystal structure data are available. Apparently the L phase is different from Q′ and eventually is replaced by Q. It is present at peak age through over age, while Q′ more often occurs with over aging. The same L phase also occurs in "Balanced + high Cu" system (0.65Si, 0.87Mg, 1Cu), but as the Cu additions increase the relative proportion of L to β″ phase at peak age increases [12]. They report that the L phase also becomes more prominent with overaging.

Precipitation in ternary excess-Si systems provides a notable contrast to that in ternary balanced systems. The β″ phase was observed present at peak age together with a lath shaped metastable phase, designated β_d'', that preferentially precipitated on dislocations [12]. This phase was replaced on over aging by a phase termed M. M, which has similar lattice parameters, crystal system (hexagonal) and morphology (lath) as the quaternary metastable phase Q′, was the only phase present on prolonged over aging (OA3). However, it was replaced later by β, the stable equilibrium phase. Matsuda et al. [16–18] reported the occurrence of a lath-shaped, orthorhombic metastable phase, denoted as Type B, on over aging which was replaced on prolonged over aging to two other metastable phases, termed Type A and Type C, in a "Ternary, Excess-Si (low)" alloy. Type C which shares similar precipitate characteristics as M and the quaternary Q′ (see Table 3) was replaced, as was M, by β the stable equilibrium phase. The metastable hexagonal phases Type A and type C were also observed by the same authors in "Ternary, Excess-Si (high)" alloys, which were replaced at equilibrium directly by the stable (Si) phase. The above studies clearly indicate that metstable phase(s) sharing the precipitate characteristics of the quaternary metastable Q′ phase can be formed in over aged ternary alloys with excess Si content. This is noteworthy, since Q has been thought to be stable only as a quaternary phase [2], while a metastable version (termed M by [12] and Type C by [16]) of it can be formed even in ternary alloys in the presence of excess Si.

As mentioned in our discussions of the equilibrium phases, the Q phase has a structure similar to that of Th_7S_{12} in which Si atoms takes the place of the Th atoms and Al and Mg atoms are randomly placed on the sites occupied by S in the prototype structure. The Cu atoms are thought to be placed at high symmetry positions. In the ternary metastable phase (M or Type C) Cu is not present, and therefore its crystal structure (lattice plus basis) is different from that of Q. The crystal system (hexagonal) and symmetry ($P\bar{6}$) of M or Type C is the same as those of Q as are the lattice parameters. For this reason it is difficult to distinguish the ternary phase from the quaternary Q phase by diffraction techniques. This ternary metastable phase is replaced on over aging by the β phase.

Detailed systematic studies including high resolution TEM by Cayron [14,15] on Al–Mg–Si–Cu alloys, derived from reactions in metal matrix composites, also revealed several metastable phases, namely the hexagonal QP at peak age, the hexagonal QC on over aging, and the hexagonal Q′ which on prolonged over aging finally led to the stable equilibrium phase, Q. Cayron has shown that the sequence of precipitation:

$$\mathrm{QP} \rightarrow \mathrm{QC} \rightarrow \mathrm{B}'(\mathrm{Q}') \rightarrow \mathrm{Q}$$

can be understood as an atomic ordering process within the basal plane of the hexagonal lattice. The *c* lattice parameter is the same for each of the phases while the *a* lattice parameter varies from that of QP to $\sqrt{3}$ times that of QP (the QC phase) to $\sqrt{7}$ times that of QP (Q′ and Q). These different phases have the same stacking sequence of the basal planes (ABAB...) but different arrangements of atoms within the basal planes. This proposal by Cayron nicely ties together the various phases reported in Table 3.

8. Strengthening phases in Al–Mg–Si–Cu alloys

Studies in the past appeared to indicate that the strengthening phase involved in the Al–Mg–Si ternary alloys is the metastable β″ phase [3,10,27,39]. The β″ phase is present at peak age while on overaging β′ and eventually equilibrium β are formed with accompanying progressive drops in strength. The prevailing viewpoint considers β″ as the most potent if not the sole strengthening precipitate in the 6xxx series automotive alloys. Thus, the increased strengthening in excess-Si alloys has been ascribed to a finer precipitation of β″ [40]. In quaternary Al–Mg–Si–Cu alloys, the strength was observed to increase progressively with increasing Cu additions. Here again the assumptions were that β″ [41] or, alternatively, β′ formed in finer sizes [39]. In what follows these interpretations will be analyzed with reference to some of our recent experimental results and the reported precipitation information in the literature.

We conducted experiments in which the hardness changes in Al–Mg–Si–Cu samples were studied as a function of artificial aging times. These changes were compared against the systematic changes in equilibrium phases and their calculated

relative amounts in samples of selected compositions. Several such groups of samples were studied, the results from two of which are presented in Figs. 8–11. Table 4 lists the compositions of two groups of samples used for the study. Fig. 8 shows the volume fraction of different equilibrium phases present at the artificial aging temperature 190 °C. These volume fractions were calculated from the equilibrium phase diagram for the compositions (a) in Table 4. Fig. 9 is a plot of the hardness (Rockwell-B)

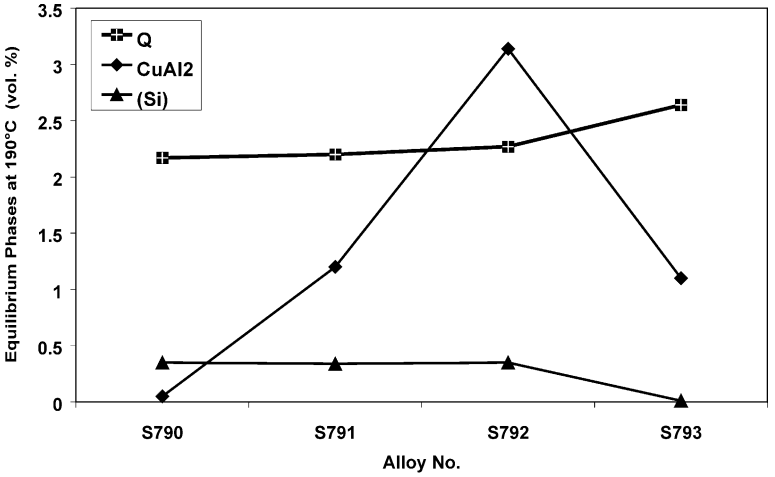

Fig. 8. Calculated volume percent of equilibrium phases at 190 °C versus composition of Al–Mg–Si–Cu alloys showing large changes in amounts of $CuAl_2$ (θ) phase.

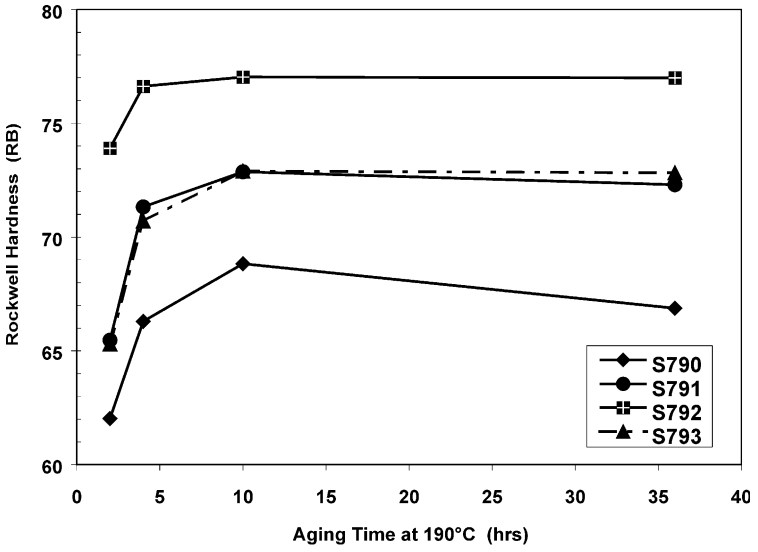

Fig. 9. Hardness changes with aging times at 190 °C for different Al–Mg–Si–Cu alloy compositions with respect to phase population changes shown in Fig. 8.

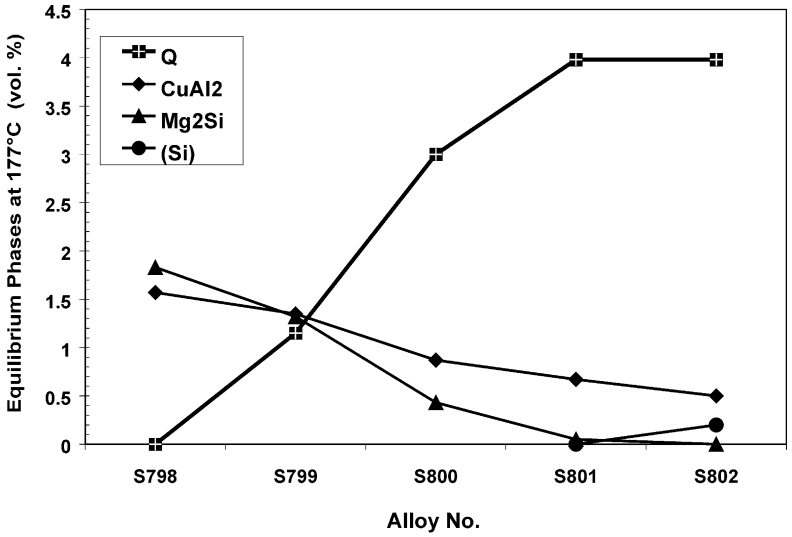

Fig. 10. Calculated volume percent of equilibrium phases at 177 °C versus composition of Al–Mg–Si–Cu alloys showing large changes in amounts of Q phase.

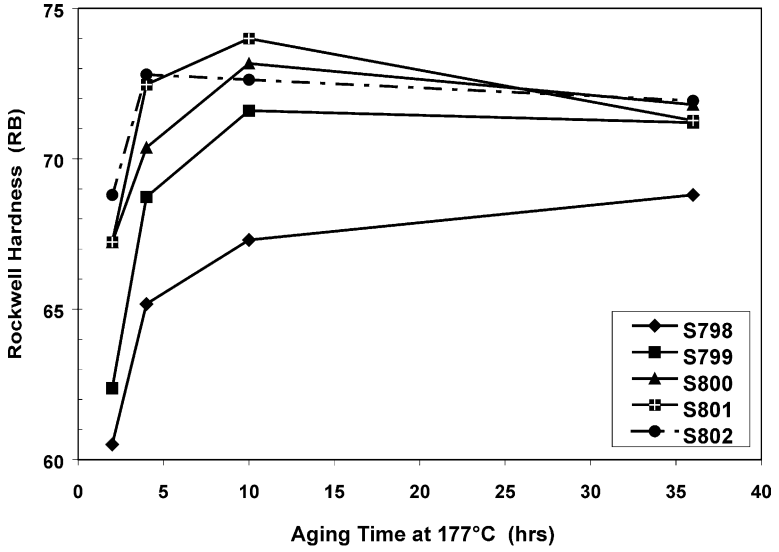

Fig. 11. Hardness changes with aging times at 177 °C for different Al–Mg–Si–Cu alloy compositions with respect to phase population changes shown in Fig. 10.

Table 4
Compositions of two groups (a, b) of samples used for hardness versus phase relations studies

(a) Specimen number	Composition (wt.%)			(b) Specimen number	Composition (wt.%)		
	Mg	Si	Cu		Mg	Si	Cu
S790	0.64	0.96	0.37	S798	1.18	0.61	0.90
S791	0.65	0.96	0.99	S799	1.17	0.81	0.93
S792	0.67	0.98	2.05	S800	1.19	1.03	0.94
S793	0.78	0.75	1.00	S801	1.20	1.13	0.95
				S802	1.22	1.36	0.88

variations with aging times at 190 °C. Prior to the artificial aging, the book mold cast ingots were subjected to the standard processing steps of homogenization, hot rolling, solution treatment, quenching and natural aging. The results show a strong correspondence between hardness values and the calculated equilibrium amount of θ ($CuAl_2$) phase. (Note, the amount of the calculated Q was similar for all the alloys.)

As the amount of θ increased (Fig. 8) the hardness also increased, see Fig. 9 samples S790 to S791 to S792. For S793, where the θ decreased so did the hardness. Even though the strengthening is not related to θ but to a precursor metastable phase, the results appear to be in conformity with the interpretation that the relative changes in the amounts of equilibrium θ reflect similar changes in the amounts of the metastable hardening phase.

Fig. 10 shows the results from another group of five compositions (compositions (b) in Table 4) selected in a way such that the calculated volume fraction of Q phase at 177 °C progressively increased with sample numbers (S798–S801) reaching a plateau, while those of β (Mg_2Si) and θ correspondingly decreased. The corresponding hardness results in Fig. 11 show a systematic increase mirroring the increase in the amount of Q phase, even though the amounts of β and θ phases, both well known for the strengthening capability of their precursor phases, decreased. Assuming that the relative amounts of the precursor phases are proportional to the relative amounts of the stable phases, and judging from the response in Figs. 8 and 9, this then offers the interesting possibility that a precursor phase of Q also has a significant strengthening capability.

Literature reports, however, indicate that the phase present at peak age in Al–Mg–Si–Cu alloys is primarily β″, while Q′ is present only during overaging and would be thus associated with decreases in strength [3,10]. Thus, the Q′ precursor phase of Q does not appear to be a strengthening phase capable of explaining the results of Fig. 11. In contrast, in one study the strength of an Al–Mg–Si balanced alloy was reported to increase progressively with increased additions of Cu. A concomitant increase in the population of a phase having rectangular cross section and containing Cu was observed in the TEM [42]. In the earlier mentioned work of Segalowicz et al. [12] with high resolution TEM, a balanced alloy with Cu additions showed the presence at peak age of a lath shaped phase, designated as L, together with the usual

β″ phase. The proportion of L increased with increased Cu addition. On overaging the L phase eventually led to another lath shaped phase which they termed λ (i.e., Q). In excess-Si ternary alloys lath-shaped phase β_d'' was also reported by the same authors at peak age [12]. High resolution TEM studies by Matsuda et al. on excess-Si ternary alloys likewise had revealed the occurrence of lath-shaped precursor phases [16]. One such metastable phase, designated Type C, was isostructural with the Q′ phase, while another phase precursor to Type C, designated Type B, was observed to occur at early stages of aging, see Table 3 [16–18]. Miao et al. [4] have also reported the existence of a lath shaped phase with habit planes parallel to {100} of Al in an alloys of both low and high Cu contents. Our high resolution TEM studies on a quaternary alloy (sample no. S802 in Figs. 10 and 11) that has a large amount of Q phase as an equilibrium phase show in near peak age conditions both the β″ precursor phase to β′ and another phase with a lath shape that is most likely the L phase identified by Sagalowicz [12], see Fig. 12. In Fig. 12(a) three precursor precipitates are shown edge on, only one of which is β″ as can be seen from Fig. 12(b) and (c) and comparing with Fig. 4 of Andersen et al. [43]. Thus, at peak age along with the normal needle-shaped β″ phase, a lath-shaped phase also is present, see Fig. 12(d) and (e). This lath shaped precursor phase of Q (which is different from the Q′ precursor phase) therefore plays a strong role on the strengthening process in quaternary alloys. The increased strengthening in quaternary alloys with Cu additions, therefore, seems to come from the L phase precursor to the Q′ phase. Thus, composition changes that show increases in the equilibrium Q phase can be indicative of corresponding increases in the lath shaped precursor phase with its significant strengthening capability. This confirms the inference of such relationships from the results in Figs. 10 and 11. According to the above results and interpretation, though neither Q or Q′ has recognizable strengthening potential, the lath-shaped precursor phases to Q′ does play a significant role in strengthening Al–Mg–Si–Cu alloys.

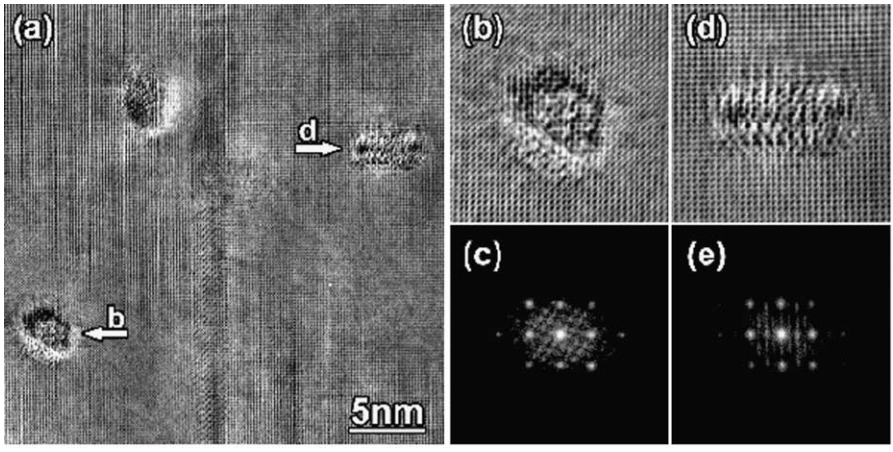

Fig. 12. High resolution TEM image of alloy S802 showing several metastable phases (a). The phase enlarged in (b) is β″ and that enlarged in (d) is a lath shaped phase similar to L. Fourier transforms of images (b) and (d) are those in (c) and (e), respectively (from [6]).

9. Summary and conclusions

1. The Al–Mg–Si–Cu alloy family incorporates many 6xxx and 2xxx alloys to which belong also many commercial and auto-body sheet alloys.
2. Many of these alloys contain the common quaternary phase Q. Often the proportion of Q is larger than the other precipitate phases at normal aging temperatures, in terms of the calculated equilibrium phase volume fractions.
3. The bulk of Al–Mg–Si–Cu alloys often occupy one of the three tetrahedron composition spaces having a four-phase equilibrium at normal aging temperatures. The phases consist of aluminum matrix, (Al), and Q as the common ones and two out of the three phases, namely Mg_2Si, (Si) or θ.
4. When the Mg/Si ratio is less than about 1, the (Si) phase is stabilized, while Mg_2Si is stabilized when Mg/Si is greater than about 1. Increasing Cu stabilizes the Q and θ phases and also increases the amount of θ.
5. Metastable version of Q, the Q′ phase, has the same crystal structure and lattice parameters as the equilibrium Q, but unlike Q it is coherent with the Al matrix along its long axis and is smaller in size.
6. Q′ has a lath morphology and a hexagonal structure, and the orientation relationship has the long axis parallel to $<100>_{Al}$ and {150} habit planes of the matrix. The lath morphology distinguishes Q′ from the needle shaped β′, the precursor of Mg_2Si.
7. Complex combinations of precursor phases, as revealed by high resolution TEM, are observed in Al–Mg–Si–(Cu) alloys as influenced by the Mg to Si ratio (balanced versus excess), the level of excess Si, the presence of Cu or the Cu level.
8. The precipitate types and forming sequences listed in the tables for the three composition groups (ternary excess Si, balanced and quaternary alloys) suggest the following:
   - A phase similar to Q′, with the same crystal system and lattice parameter as Q (termed either M or Type C), can be formed in excess-Si ternary alloys (without Cu), but is metastable. On overaging, it is replaced by β and/or (Si) instead of forming an equilibrium Q like phase as in the quaternary system.
   - Similar to β′ having the precursor phase β″, precursor phases with a lath morphology exist for the Q′ phase, for example "L" for quaternary and β_d'' for ternary excess Si compositions.
9. In Al–Mg–Si–Cu quaternary alloys, significant strengthening effects may arise from the lath shaped, hexagonal precursor phases to Q′ in addition to the generally recognized β″ phase.

Acknowledgements

D.J.C. wishes to thank Alcoa management for supporting a part of the work reported and for the approval to publish the paper. D.E.L. acknowledges the help of

Dr. Byung-ki Cheong, Dr. Weifeng Miao and Dr. Yingguo Peng, as well as the financial support of Ford Motor Company.

References

[1] Dumolt SD, Laughlin DE, Williams JC. Scripta Met 1984;18:1347.
[2] Chakrabarti DJ, Cheong BK, Laughlin DE. In: Das SK, editor. Automotive alloys. Warrendale (USA): TMS; 1998. p. 27.
[3] Miao WF, Laughlin DE. Scripta Mat 1999;40:873.
[4] Miao WF, Laughlin DE. Met Mat Trans 2000;31A:361.
[5] Miao WF, Laughlin DE. J Mat Sci Letters 2000;19:201.
[6] Chakrabarti DJ, Peng Y, Laughlin DE. Intl Conf of Al Alloys 8. Cambridge (UK): Cambridge University; 2002.
[7] Hardy HK, Heal TJ. Progress in Metal Physics 1954;5:143.
[8] Kelly A, Nicholson RB. Progress in Materials Science 1963;10(3).
[9] Thomas G. J Inst Met 1961–1962;90:57.
[10] Edwards GA, Stiller K, Dunlop GL, Couper MJ. Acta Mat 1998;46:3893.
[11] Phragmen G. J Inst Metals 1950;77:489.
[12] Sagalowicz L, Hug G, Bechet D, Sainfort P, Lapasset G. Intl Conf of Al Alloys 4. Switzerland: Trans Tech; 1994. p. 636.
[13] Perovic A, Perovic DD, Weatherly GC, Lloyd DJ. Scrip Met 1999;41:703.
[14] Cayron C. These No. 2246. Ecole Polytech. Fed., Lausanne, 2000.
[15] Cayron C, Sagalowicz L, Beffort O, Buffat PA. Phil Mag 1999;79:2833.
[16] Matsuda K, Ikeno S, Sato T, Kamio A. Mater Sci Forum 1996;707:217–22.
[17] Matsuda K, Uetani Y, Sato T, Ikeno S. Met and Mat Trans 2001;32A:1293.
[18] Matsuda K. Private communication.
[19] International alloy designations and chemical composition limits for wrought aluminum and wrought aluminum alloys. Washington (DC, USA): The Aluminum Association, January 2001.
[20] Dix EH, Sager GF, Sager BP. Trans Amer Inst Min Met Eng 1932;99:119.
[21] Crowther J. J Inst Metals 1949–1950;76:201.
[22] Axon HJ. J Inst Metals 1952–1953;81:209.
[23] Collins DLW. J Inst Metals 1957–1958;86:325.
[24] Smith DP. Metallurgia 1961;63:223.
[25] Petrov DA. Acta Physico Chimica URSS 1937;VI(4):505.
Petrov DA, Nagorskaya ND. Zhur Obschey Khimi 1949:1994.
[26] Philips HWL. Equilibrium diagrams of aluminium alloy systems. London: The Aluminium Development Assoc; 1961. p.128.
[27] Suzuki H, Araki I, Kanno M, Ito K. J Japn Inst Metals 1977;27(5):239. Japanese.
[28] Stumpf HC. Alcoa proprietary internal data.
[29] Edwards GA, Dunlop GL, Couper MJ. Intl Conf of Al Alloys 4. Switzerland: Trans Tech; 1994. p. 620.
[30] Chakrabarti DJ. Alcoa unpublished results.
[31] Arnberg L, Aurivillius B. Acta Chem Scand Series A 1980;34A:1.
[32] Wolverton C. Acta Mat 2001;49:3129.
[33] Villars P, Calvert LD, editors. Pearson's handbook of crystallographic data for intermetallic phases, vol. 1, 2nd ed. OH (USA): ASM; 1991. p. 769.
[34] Mondolfo LF. Aluminum alloys: structure and properties. Boston: Butterworths; 1979. p. 644–51.
[35] Gupta AK, Jena AK, Chaturvedi MC. Mater Sci Tech 1987;3:1012.
[36] Eskin DG. Z Metallkd 1992;83:762.
[37] Khachaturyan A. Theory of structural transformation in solids. Wiley Interscience; 1983.
[38] Sagalowicz L, Lapasset G, Hug G. Phil Mag Lett 1996;74(2):57.

[39] Sakurai T, Eto T. Intl Conf of Al Alloys 3. Switzerland: Trans Tech; 1992. p. 208.
[40] Matsuda K, Terasaki M, Tada S, Ikeno S. J Jpn Inst Light Metals 1995;45:95.
[41] Laughlin DE, Miao WF, Karabin LM, Chakrabarti DJ. In: Das SK, editor. Automotive alloys. Warrendale (USA): TMS; 1998. p. 63.
[42] Tamizifar M, Lorimer GW. Intl Conf of Al Alloys 3. Switzerland: Trans Tech; 1992. p. 220.
[43] Andersen SJ, Zandbergen HW, Jansen JJ, Traeholt C, Tundal U, Reiso O. Acta Mat 1998;46:3283.